Quinic acid as a novel depressant for efficient flotation separation of scheelite from calcite

Zheyu Huang [1,2], Jingzhong Kuang [1,2], Mingming Yu [1,2], Dan Ding [1,2]

[1] Jiangxi Key Laboratory of Mining Engineering, Ganzhou, 341000, China

[2] School of Resource and Environmental Engineering, Jiangxi University of Science and Technology, Ganzhou, 341000, China

Corresponding author: kjz692@163.com (Jingzhong Kuang)

Abstract: There are difficulties to the conventional depressant for achieving separation of scheelite from calcite for the sake of their similar surface properties. The paper reported that a new depressant quinic acid (QA) was used for separating scheelite from calcite. The adsorption experiments, zeta potential experiment, contact angle, FTIR, XPS analysis and crystal chemistry analysis were utilized to known the depression mechanism of selectivity. The results showed that the recovery of calcite decreased drastically after QA added, whereas hardly influenced on scheelite. The tungsten concentrate could reach 66.24% WO_3 grade and 89.46% recovery with 1.5×10^{-4} mol·L^{-1} QA at pH=9. The surface adsorption quantity of the QA on calcite was much greater than scheelite, which enhanced significantly the hydrophilicity of calcite surface. Due to its negative charge, QA could be adsorbed on the surface of calcite which had positive charge instead of that of scheelite with negative charge. Subsequently, free carboxyl groups of QA could chelated with Ca^{2+} species on the calcite surface to form stable chemical adsorption in order to prevent the Pb-BHA to form further adsorption on that, so there was no increase significantly on hydrophobicity. However, QA was obviously weak for adsorbing while Pb-BHA which could still be chemically adsorbed on scheelite surface of pre-treated with QA.

Keywords: quinic acid, scheelite, calcite, depression, selective adsorption

1. Introduction

Tungsten is a rare metal as well as a strategic metal (Gong et al., 2022). As the main source of tungsten resources, the exploitation and utilization of scheelite has attracted much attention from researchers (Yang, 2018). The key to improve the utilization level of scheelite resources lies in the flotation separation of scheelite from calcium-containing minerals (Kupka and Rudolph, 2018; Kalpakli. et al., 2012). Scheelite and calcium-containing minerals have the same surface active sites and similar surface dissolution characteristics, which makes scheelite and calcium-containing minerals difficult to separate effectively (Han et al., 2020; Lu et al., 2014; Shepeta et al., 2014). Calcite is a kind of low-price gangue mineral often associated with scheelite. Calcite has high solubility, low density, good solubility, easy to be crushed and easy to adhere to the bubble. Therefore, it is more difficult to separate scheelite from calcite by flotation.

The selectivity of depressants is a crucial factor in the flotation separation of scheelite from calcite (Wang and Ren et al., 2021; Han et al., 2018; Liu et al., 2021). At present, the flotation of scheelite and calcite mainly consists of inorganic depressants such as sodium silicate (Foucaud et al., 2019), sodium fluorosilicate (Dong et al., 2019b), sodium hexametaphosphate (Kang et al., 2019), sodium triphosphate (Wang et al., 2021), etc. However, organic depressants have the advantages of wide sources, multiple types, convenient design, simpleness to synthesis, stronger ability to restrain, easily degradable, and little environmental pollution, which have attracted more and more researchers' attention. Organic depressants can be divided into small molecule and macromolecular depressants (Li et al., 2011; Dong et al., 2021a; Sarquís et al., 2014). Small molecule organic depressants mainly include citric acid (Dong et al., 2021a), tartrate (Zhang and Sun et al., 2018), salicylic acid (Han et al., 2020), oxalic acid (Nuri et

al., 2019), etc. Small molecule depressants have fairly water solubility and low viscosity but weak inhibition and selectivity which achieves the inhibition effect by combined utilization (Dong et al., 2021c). Carboxyl group has strong hydrophilicity and reaction activity which is the main hydrophilic group of small molecule depressants (Fu et al., 2021; Wang et al., 2018; Dong et al., 2019b; Jiao et al., 2019; Chen et al., 2018; Dong et al., 2018). But the depressants can adsorb not only on the surface of calcite but also on scheelite because of the more carboxyl functional groups, resulting in poor selectivity of small molecule depressants. In recent years, macromolecular polymers have been found to the depression effect on flotation. For example, the sodium alginate, CMC, pectin, xanthan gum, etc. can selectively inhibit calcite in scheelite flotation. Most of the macromolecular depressants have better selectivity than the small molecular depressants and better selective separation of scheelite from calcite. The macromolecular depressants contain not only carboxyl groups, but also a large number of hydroxyl functional groups. Carboxyl groups in the molecule interact with Ca atoms on the surface of minerals to form chemical adsorption (Zhang et al., 2019; Liu et al., 2022). Hydrophilicity of depressants is mainly provided by hydroxyl groups in the molecule. The macromolecular depressants with the disadvantages of poor water solubility and high viscosity would be enriched in the process of mineral flotation cycle, resulting in too high slurry viscosity, deterioration of flotation index and unfavorable recycling of wastewater. It is significant to find a small molecule depressant with low viscosity, good selectivity, more polyhydroxy and few carboxyl groups in the molecule to realize the industrial application of organic depressants.

Quinic acid which coexists frequently with shikimic acid in vascula plants commonly is an unique alicyclic organic acid of higher plants and a precursor of aromatic amino acid biosynthesis (Samimi et al., 2021; Holmstedt et al., 2021). Quinic acid with the multiple chiral centers structure is significantly and widely serves as a chiral raw material in stereo-organic synthesis to synthesize natural products and prepare new polymeric materials (Gabriel et al., 2008; Clifford et al., 2017). Quinic acid molecule only has one active carboxy, its hydrophilic group is mainly hydroxyl group, which not only has oligo-carboxyl polyhydroxy structure of polymer depressants, but also has the advantages of small molecule depressant fairly water solubility and low viscosity with a small molecular weight. However, the role of quinic acid on floating and separating scheelite from calcite haven't been reported and known. So this paper analyzed single as well as artificial mixture minerals flotation in order to know the effects of quinic acid on floating and separating scheelite from calcite, and particularly accounted for the interaction mechanism of minerals and quinic acid with contact angle, zeta potential, FTIR spectroscopy, XPS analysis and crystal chemistry analysis.

2.   Materials and methods

2.1.   Experimental materials

The scheelite and calcite took in the experiment were taken from a mine in Sichuang Province, China. The scheelite and calcite samples with a particle size of -74 μm ~ +37 μm were obtained by crushing-grinding-screening, which was utilized for microflotation and adsorption experiments. The fine particle (-37 μm) was unceasingly ground to less-than 5 μm for zeta potential experiment and analyses of FITR, X-ray diffraction (XRD), X-ray fluorescence (XRF) and chemistry. According to the XRD (D8 advance X-ray diffractometer, Brucker company) results in Fig. 1, the diffraction peaks of scheelite and calcite corresponded respectively to the standard pattern of scheelite (PDF#72-0257) and calcite (PDF#72-1937) without that of other substances. The XRF (ARLAdvantx IntelliPower TM3600 X-ray fluorescence spectrometer, Thermo Fisher company) analysis results of scheelite shown that the total content of O, Ca, and W exceed 98% in Table 1, and that of calcite explained that the total impurity content of main elements of O and Ca was less than 2% in Table 2. The XRD and XRF analysis results confirmed that these minerals had good crystallization and high purity. The grade of WO_3 in scheelite is 78.87% and that of $CaCO_3$ in calcite is 98.89% through chemical analyses, which could meet the requirements of experiments. The artificially mixed minerals were prepared by mixing scheelite and calcite particles at a mass ratio of 1:1, and artificially mixed minerals presented that the WO_3 content was 39.13% via chemical analyses.

The main reagents with analytically pure used in the experiment include benzohydroxamic acid (BHA) and methyl isobutyl methanol (MIBC) (Shanghai Aladdin Biochemical Technology Co., Ltd.,

China), hydrochloric acid, sodium hydroxide and lead nitrate (Sinopharm Chemical Reagent Co., Ltd., China), quinic acid (QA, Shanghai McLean Biochemical Technology Co., Ltd., China). The molecular structure of QA was shown in Fig. 2. The experiment water was ultrapure water.
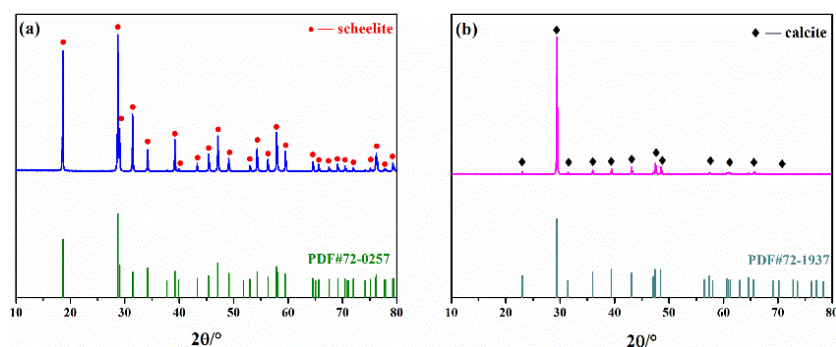
Fig. 1. XRD pattern of scheelite (a) and calcite (b) as raw materials

Table 1. XRF results of semiquantitative element content (%) in scheelite

O	Ca	W	Na	Al	Si	P	S	Cl	K	Sr	Y	Nb
21.399	13.381	63.79	0.045	0.306	0.603	0.108	0.083	0.032	0.113	0.08	0.032	0.028

Table 2. XRF results of semiquantitative element content (%) in calcite

O	Ca	Mg	Al	Si	P	S	Cl	Mn	Fe	Sr	Bi
33.69	48.281	0.158	0.015	0.031	0.001	0.012	0.019	0.013	0.013	0.004	0.004

2.2.   Experimental methods

2.2.1.   Microflotation experiments

It was sought whether the depressant QA acted on floating scheelite from calcite in the microflotation experiments which were conducted with an XFG flotation machine (Jilin Exploration Machinery Plant, Changchun, China) with a capacity of 40 mL at speed of main shaft at 1758 rpm. It needed to add 2.0 g mineral samples into 35 mL of ultrapure water and agitated for 3 min for suspending mineral. The slurry pH was first adjusted by adding NaOH or HCl solution for 3 min before adding in depressant QA of varying concentration for 3 min. Then, the collector Pb-BHA complex by Pb^{2+} and BHA in a molar ratio of 1:1 was allowed to react for 3 min，the concentration of Pb-BHA complex in the slurry was 1.5×10^{-4} mol·L^{-1}. Then the MIBC would be added into slurry for 3 min and the concentration of MIBC in slurry was 0.5×10^{-4} mol·L^{-1}. Finally, the collection, drying and weighing of concentrate and the tailing were finished to calculate. The recovery was calculated according to Eq. (1):

$$\varepsilon = \frac{m_1}{m_1+m_2} \times 100\% \tag{1}$$

where ε is the recovery; m_1 is the concentrates products weight (g); m_2 is the tailing products weight (g).

The actual separation effect with the addition of depressant and the effect without that on scheelite from calcite were explored by the artificial mixed mineral experiments. Each experiment needed weighing 4.0 g of mixed samples, the reagent's sequence of addition and reaction time in the process of experiment were as same as the flotation experiment on single mineral. When the flotation was accomplished, the flotation froth and tailing were gathered separately to figure up the yield and analyze the grade of WO_3 in concentrates and tailings as well as computed the scheelite's recovery successively. Each condition experiments of single-mineral and artificial mixed mineral flotation obtained the average value after 3 times of repetition.

2.2.2. Adsorption experiments

The residual concentration method was applied to survey adsorption quantity of QA on the scheelite and calcite surface under different reagent conditions. 2.0 g of mineral samples and 40 mL of ultrapure water was placed in a plexiglass cell. First, then adjust the pH of the slurry by adding NaOH or HCl

solution. Secondly, the depressant QA was added in the slurry to react for 40 min for getting the completely surface adsorption of flotation reagent on the mineral. Finally, solid-liquid separation of the slurry was completed by centrifuge at 8000 r/min for 10 min. The concentration in the supernatant were measured by TOC analyzer (HTY-DI1500 TOC, Germany Jena Analytical Instruments Co.) and the surface adsorption quantity of QA on scheelite or calcite were calculated by Eq. 2. The average value and standard deviation were counted after five adsorption capacity tests at every condition.

$$\Gamma = \frac{(C_0\text{-}C)V}{m} \tag{2}$$

where C_0 is the initial and C is the supernatant concentrations of the flotation reagents, separately (mol·L^{-1}); V is the solution volume (L); m is the mineral's weight (g).

2.2.3. Zeta potential experiments

The experiment which was proceed on a Zetasizer Nano ZS90 analyzer (Malvern Instruments Ltd.) had been selected a certain concentration of potassium nitrate solution to be the background electrolyte. During the experiment, a certain amount of pure mineral samples (particle size: -5 μm) were added into the beaker with the electrolyte solution meantime to get 0.1% of slurry concentration which was stirred with a magnetic stirrer subsequently. The values of zeta potential could be known via taking the stable suspension after adding relevant reagent in line with the flotation process. The average value and standard deviation would be valued by trials for each condition with 5 times of repetition.

2.2.4. Contact angle experiment

The surface of each block-shaped mineral sample which cut to be regular parallelepipeds and made a fixation through resin firstly was polished with machine from coarse to fine until it is smoothly to ready for water contact angle analysis. Before the experiment, the repeating washing with ultrapure water to wipe off superficial contaminants of minerals and the 20-minute treatment in flotation reagent solution were needful. The concentration of reagent and its pH acting with mineral were consistent with the conditions of flotation test. After the reaction, the mineral sample needed to proceed extraction, repeating rinse with distilled water and dry with ultrapure nitrogen. An automatic sample injection syringe which is used to drop the blob of ultrapure water on the mineral surface and a contact angle meter (KRUSS DSA1005 of German) which is served for measuring the contact angle after the stable formation of the blob were utilized.

2.2.5. FTIR analysis

The FTIR spectra of scheelite and calcite with the presence or absence of QA and Pb-BHA complex system were estimated with Bruker ALPHA FTIR spectrometer of Germany. The reaction for 120 min of 2.0 g of mineral samples (particle size: -5 μm) with reagents was at work in accordance with the dosing sequence of microflotation tests. Then, the filtered sample would be vacuum-dried thoroughly after being scoured below 50°C for FTIR spectra collection. The dispersion of dried sample with an agate mortar would be done for the measurement in KBr whose ratio with sample was about 1:100. The records of spectrum in the range from 400 cm^{-1} to 4000 cm^{-1} were get with a 1 cm^{-1} resolution in each test.

2.2.6. XPS analysis

The chemical state and environment of elements on the surface of mineral which reacted with the reagent was sook by XPS including that of elements without reaction. With adding 2.0 g of the minerals (particle size: from -74 μm to +38 μm), the XPS tests which wouldn't be added the QA solution until pH was adjusted was performed in the flotation cell for 60 min. The mineral samples needed the processes of reduplicative rinse with deionized water, filter, and dry in a vacuum oven to do experiment. The experiments were worked by utilizing ESCALAB 250Xi (Thermo Fisher, the United States) with monochromatic Al Ka X-ray source at 150 W. The energy step sizes of surveying and high-resolution XPS spectra were 1.00 and 0.05 eV, respectively. Particularly, C 1s is applied to calibrate the all elements at 284.8 eV.

3.   Results and discussion

3.1. Effects of QA on flotation of scheelite and calcite

The floatability of scheelite and calcite under the depressant QA and the collector Pb-BHA complex system is seen in Fig. 3. Fig. 3(a) showed the role of slurry pH on the flotation recovery of the two minerals. The scheelite had very high floatability with calcite which are better to lack of the depressant. The recovery of scheelite was gradually improved in the pH range of 7.0~10.0 (from about 66% to exceed 95%) while its recovery rate was less than 20% at pH=12 of the slurry because the recovery of scheelite and calcite decreased drastically at high pH (10.0~12.0). Therefore, the flotation separation of the two minerals was impossible to achieve without adding a depressant, especially at low pH studied (7.0~9.5). Even if the addition of QA made the floatability of the minerals was inhibited, the QA was still hard to impact on the recovery of the scheelite at the slurry pH from 7.0 to 10.0 for its weak inhibitory effect on scheelite. In comparison, in the presence of QA, calcite was extensively suppressed and its recovery had a sudden drop in the pH range of 7.0~9.0 (from about 50% to less than 20%). So we could know that there were high possibility about floating as well as separating scheelite from calcite with the help of QA.

The study of role of QA concentration on the flotation recovery of scheelite and calcite was conducted at pH = 9.0. As the Fig. 3(b) shown, the scheelite and calcite had higher recovery (over 80%) without the additive depressant. However, the recovery of calcite was decline with the QA concentration upped but that of scheelite almost remained unchanged. With addition of depressant QA concentration was $0\sim3.0\times10^{-4}$ mol$\cdot$L^{-1}, the scheelite could still be floated which recovery almost above 80%. When QA concentration was increased to 1.5×10^{-4} mol$\cdot$L^{-1}, calcite downed to 20.01% while scheelite still kept higher concentrate of 95.53%. Moreover, the highest difference in recovery between scheelite and calcite could occur about 70.0% at QA concentration=1.5×10^{-4} mol$\cdot$L^{-1} which was proved to be the optimal concentration of depressant. It could be seen that QA had good selectivity to depress calcite and make the flotation separation of scheelite and calcite better.
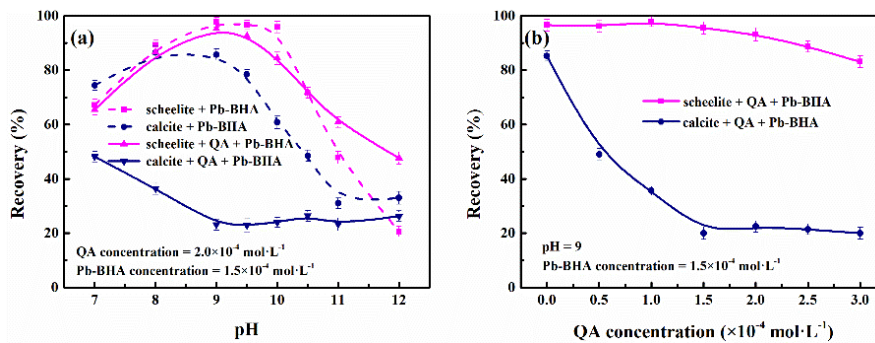
Fig. 3. Role of QA in single mineral flotation of scheelite and calcite, (a-pH; b-QA concentration)
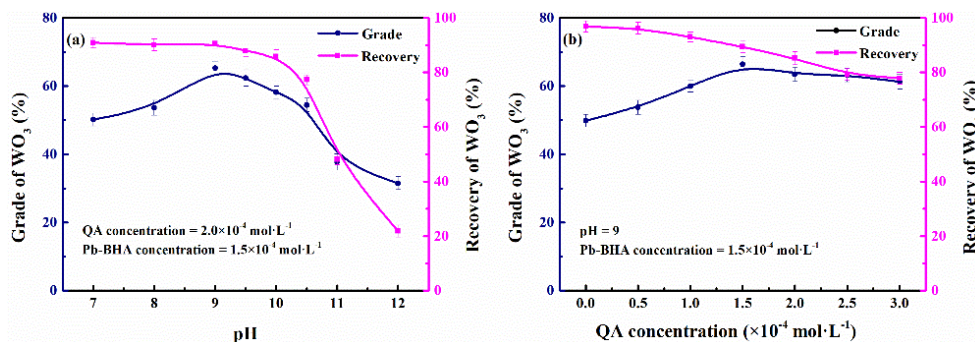
Fig. 4. Role of QA in separation of scheelite from calcite, (a-pH; b-QA concentration)

The results of artificial mixed mineral experiments which confirmed the impact of the QA on the two minerals are exhibited in Fig. 4. The changes of WO$_3$ grade and recovery of flotation foam products with pH values in the presence of the depressant QA are shown in Fig. 4(a). The grade of WO$_3$ which

exceeded 65% from about 50% was gradually increased in the pH range of 7.0~9.0, whereas its recovery which was about 90% was hardly influenced. The grade and recovery of WO_3 decreased drastically with constant increase of the slurry pH (9.5~12.0). When the slurry was at pH=9, The grade of concentrate was 65.29% and the recovery was 90.58%, which indicated that pH=9 was the optimal pH for flotation. The flotation grade and recovery of WO_3 at various QA concentration were shown in Fig. 4(b). Without depressant, the WO_3 grade of the gained concentrates was 49.85%, which was only slightly above that of the raw ore which was 39.13%. So there were hardness to get efficient enrichment of scheelite with merely adding the collector Pb-BHA complex. However, when the depressant QA was added in advance, the grade of WO_3 was improved with the increase of QA concentration, whereas the recovery of WO_3 was slightly reduced. Although the recovery of WO_3 in the concentrates had dropped slightly from 96.84% to 89.46% at 1.5×10^{-4} mol $\cdot L^{-1}$ of QA concentration, the grade of WO_3 in the concentrates had been greatly increased to 66.24%. This indicated that the separation efficiency of scheelite and calcite was greatly improved, and the selectivity of the depressant QA had been proven.

3.2.1. Adsorption experiment results

Its surface adsorption quantity exhibited the intuitive characteristics on the influence of flotation reagents on mineral floatability. The Fig. 5. shown that the adsorption quantity of QA on the scheelite and calcite surfaces increased with the initial concentration of QA which was at a fixed pH=9. Although the amounts of surface adsorption of depressant QA on the calcite was considerable, its quantity of that on the scheelite was extremely low. Thus, it could be known that the QA played stronger inhibiting role on calcite than scheelite for the sake of significant reduction of floatability of calcite.
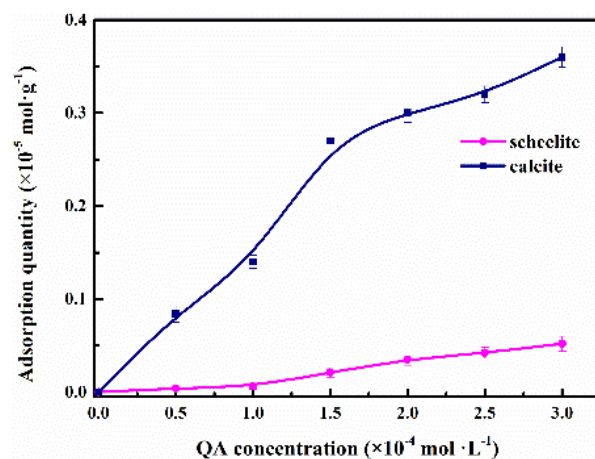
Fig. 5. Adsorption quantity of QA on scheelite and calcite surfaces

3.2.2. Wettability

The wettability of the surface which determined the floatability of the mineral could be changed with the flotation reagent acting. As seen as Fig. 6, the surface water contact angles of untreated scheelite and calcite samples were 39.6° and 36.9° severally which indicated that they had similar and poor floatability, but the angles would increase sharply to 88.4° and 70.4° with the treatment of Pb-BHA complex on the samples. The changes of the angles proved their hydrophobicity and floatability had obvious improvement, which made the two minerals would float up at the same time resulting in the failure on separating scheelite from calcite. The contact angle slightly downed to 34.9° with QA acted on the scheelite sample, it made clear that QA existed limitation to adsorb on the scheelite surface. In comparison, the reaction that QA on the surface of calcite realized that the contact angle reduced extremely to 13.7°, illustrating that QA was significantly adsorbed on the calcite surface. Finally, the two minerals had reaction with QA following with Pb-BHA, which given the phenomenon that the surface of scheelite still exhibited a relatively high contact angle of 81.2° and that of calcite was only 28.6°, that performed the stronger hydrophobicity and floatability on scheelite and obviously the weaker on calcite, for that the selectivity of QA to adsorb on the surface of calcite stopping the farther adsorption of Pb-BHA.
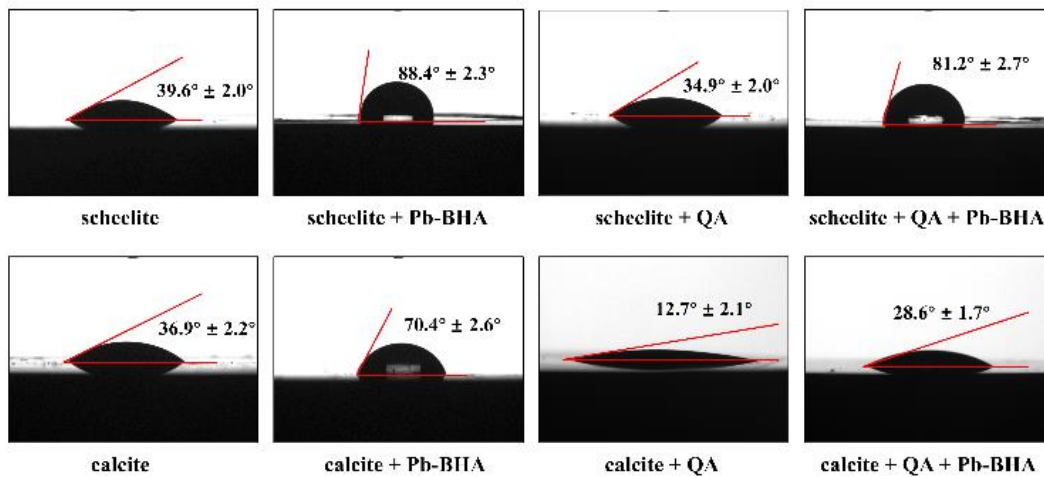
Fig. 6. Role of QA in contact angle of mineral surface

3.2.3. Zeta potential

The influence of values of zeta potential of minerals which tested at various pH with QA and Pb-BHA was used to study the role of QA playing on the Pb-BHA to adsorb on mineral surfaces. The variations which have the reaction and no reaction with the reagent in zeta potential on the minerals surface could be seen Fig. 7. The Fig. 7 (a) shown the negative values of zeta potentials of scheelite at pH=7.0~12, and Fig. 7 (b) exhibited the isoelectric point (IEP) of calcite at pH=9.21, which was consistent with previous literature studies (Kang et al., 2019; Gao et al., 2016). The depressant QA appeared negative charge through the test pH range, which indicated that QA had electrostatic repulsion with scheelite and electrostatic attraction with calcite at pH<9.21. The slight shifts of charge by treating with QA which was explained it was hard to play a part in scheelite surface charge. Whilst, the further distinct transforms to negative charges appeared in the calcite surface (Fig. 7 (b)), it indicated that the strong surface adsorption on the calcite arisen with negative charge of QA. The rising magnitude of the zeta potential on the scheelite was higher than that of calcite on the surfaces when the collector Pb-BHA was added to the slurry formed by pre-adsorbed depressant QA, indicating that the collector had strong surface adsorption on the scheelite but the inapparent on calcite.
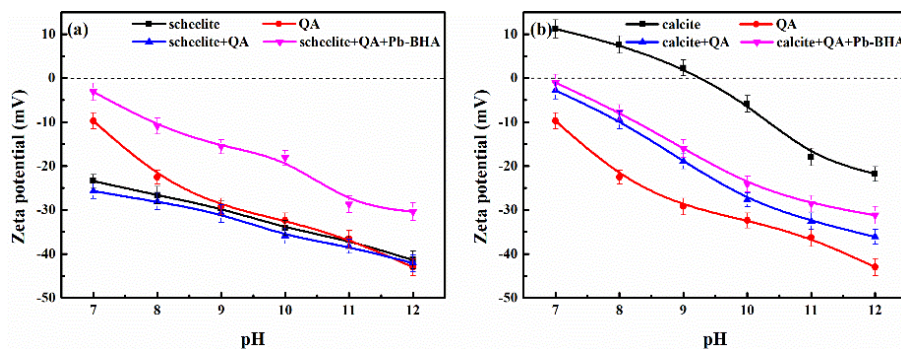
Fig. 7. Zeta potential of scheelite (a) and calcite (b) with the treatment of QA and Pb-BHA

3.2.4. FTIR analysis

The analyses of the infrared spectra before and after the reaction with the flotation reagent on the surface of the minerals were given to know the reagent's adsorption mechanism. The infrared spectra of QA and Pb-BHA complex are shown in Fig. 8. As the paper discussed in infrared spectra of Pb-BHA, the characteristic peak at 3682 cm^{-1} was thought as the hydroxyl group peak and the peaks at 3300 cm^{-1}, 3060 cm^{-1}, 2805 cm^{-1}, 1621 cm^{-1}, and 1154 cm^{-1} was apart taken for the stretching vibrations of partial overlap of N-H and O-H and N-H, O-H, C=O, C-N (Han et al., 2020). The vibration of C-C in the benzene ring made the peaks arise at 1566 cm^{-1} and 1386 cm^{-1}. The bending vibration of C-H were happened at

the wavenumber of 908 cm^{-1}, 792 cm^{-1}, and 688 cm^{-1} (Wei et al., 2018; Saldyka and Coussan, 2020). Seeing the infrared spectra of QA, the stretching vibration of hydroxyl group peaks were typical at 3527 cm^{-1}, 3395 cm^{-1}, 3339 cm^{-1} and that of C-H in QA was remarkable at 2975 cm^{-1} and 2932 cm^{-1}, that of unesterified carboxyl (-COO-) was obvious at 1683 cm^{-1} and 1451 cm^{-1} (Espiritu et al., 2018), similarly, that of C-O stretching vibration peak was prominent at 1055 cm^{-1}. While the bending vibrations of C-H were at the wavenumber of 922 cm^{-1} and 801 cm^{-1} as well as the out-of-plane of O-H was at the peak of 660 cm^{-1} (Allegretti et al., 2000).
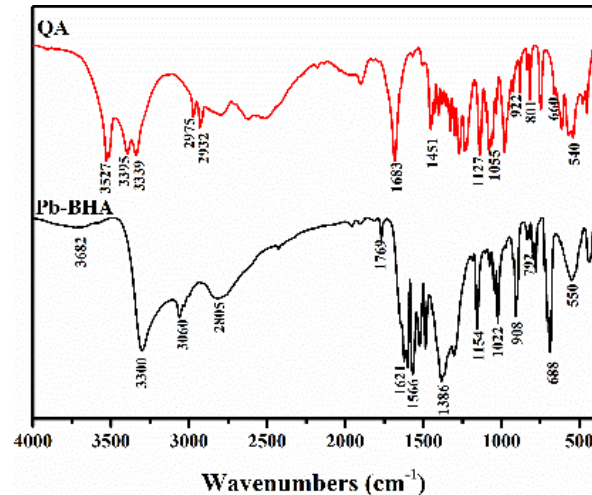
Fig. 8. FTIR spectrum of Pb-BHA and QA

The Fig. 9(a) show the changes in the infrared spectra of the scheelite when the reactions with reagents were took or not yet, the Fig. 9(b) show that changes of calcite under the same conditions. The characteristic peaks which belonged to the scheelite of the stretching and the bending vibrations of the W-O bonds of CaWO$_4$ were respectively at 806 cm^{-1} and 440 cm^{-1} from Fig. 9(a) (Abdalla et al., 2018; Dong et al., 2019b). The differences when the scheelite reacted respectively with Pb-BHA complex and QA could be observed. With Pb-BHA, the stronger chemical adsorption of the complex on the scheelite surface could be indicated because the benzene rings peak was at 1384 cm^{-1} (Wei et al., 2021), while with QA, the weak of QA was indicated because the peak had little changes and didn't appear the new characteristic one. Even if the scheelite had reaction with QA and Pb-BHA in sequence, there are only the characteristic peak of Pb-BHA, so the weak adsorption of QA did not prevent the strong of Pb-BHA. As seen as from Fig. 9(b), the peak of stretching vibration of C-O in calcite appeared at 1430 cm^{-1}, and the bands which was caused by its deformation vibration were at 876 cm^{-1} and 712 cm^{-1} (Katelnikovas et al., 2017). In the presence of collector Pb-BHA complex, the new absorption peaks arisen at 1154 cm^{-1}, which was corresponded the C-N stretching vibration peak of Pb-BHA (Wei et al., 2020). With the depressant QA interacted on calcite, there are new significant absorption peaks at 1051 cm^{-1} on calcite surface (Fig. 9(b)), which resulted from the stretching vibration of the C-O group in depressant QA (Samimi et al., 2021). So the chemisorption of depressant QA was strong on calcite but that on scheelite was extraordinary weak (Fig. 9(a)). When the depressant QA and collector Pb-BHA presented commonly, the other absorption peaks didn't arise except peaks of stretching vibration of QA (1051 cm^{-1}) which accounted the pre-adsorption of QA hindered the adsorption of Pb-BHA on calcite surface. The results of FTIR analysis further verified that the QA paly the selective role of depression on calcite.

3.2.5. XPS analysis

For investigating the adsorption effect of QA on the scheelite and calcite, changes of the surface properties of that before and after the addition of QA were analyzed by using XPS. The XPS survey spectra of QA-adsorbed scheelite and calcite samples as well as their semiquantitative atomic concen trations is showed from Fig. 10. The Fig. 10(a-I) and Fig. 10(b-I) showed respectively that the scheelite only contained C, O, Ca and W elements and the calcite only had C, O and Ca elements, indicating that the two kinds of samples had a high purity. After adding QA to scheelite and calcite, the atomic concentrations of C and O on the surface of scheelite each augmented merely by 0.77% and 0.02%, while
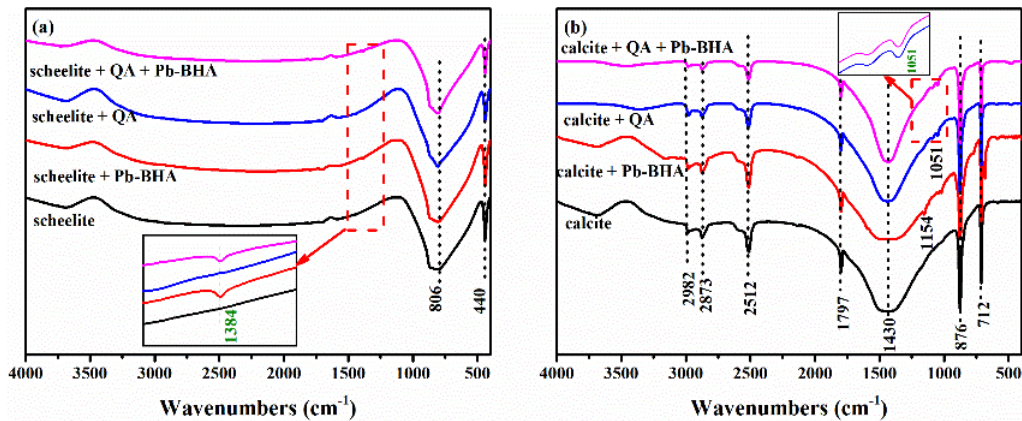
Fig. 9. FTIR spectra of scheelite (a) and calcite (b) before and after the reaction of reagents

that of calcite each upped by 3.37% and 0.50%. This result suggested that adsorption amount of QA onto calcite was lager but that on scheelite was faint. The reduction of content of Ca atoms on the minerals surface indicated that QA adsorbed on the scheelite and calcite surface to cover Ca atoms on the minerals surface.

XPS high-resolution spectra of C1s, O1s and Ca2p to analyze more deeply the adsorption of QA on minerals surfaces before and after adding QA are shown in Fig. 11 to Fig. 13. From Fig. 11, without the role of QA, the two peaks separated at ~284.79 eV and ~286.25 eV in Fig. 11(a-I) resulted from forming hydrocarbon and carbon oxide contaminants on the scheelite surface (Deng et al., 2018; Chen et al., 2017). The three divided peaks were at ~284.80 eV, ~286.31 eV and ~289.68 eV in high-resolution spectrum of C1s on calcite surface in Fig. 11(b-I) (Feng et al., 2018; Zhang et al., 2018), which was well-matched with hydrocarbons, carbon oxides contaminants and the carbon in the carbonate of the calcite ($CaCO_3$), respectively. After interaction of scheelite and calcite with QA, there were only hydrocarbons and carbon oxides with separated peaks at ~284.77 eV and ~286.07 eV on the surface of scheelite (Fig. 11(a-II)) without new peaks, while there was new separated peak at ~287.76 eV on the surface of calcite (Fig. 11(b-II)), which belonged to O=C-O (Martins et al., 2018; Jin et al., 2016). It was clear that the carboxyl group in the QA molecule was able with calcite but difficult with scheelite to chelate with the calcium ion on the surface. From Fig.12 which could be seen the high-resolution spectrum and separated and fitted peaks of O1s on the surfaces of scheelite and calcite, the spectrum of O1s (Fig. 12(a-I)) was divided into two peaks of ~530.37 eV and ~531.32 eV, representing the metal oxides compounds (W-O, $CaWO_4$) which was in scheelite and the carbon oxygen pollutants (Yao et al., 2022), while the peaks of O1s (Fig. 12(b-I)) for calcite were separated at ~531.49 eV and ~532.26 eV, which were the oxygen in CO_3^{2-} of calcite ($CaCO_3$) and carbon oxides contamination (Liu et al., 2015). After reaction with QA, there were no new peak meant no clear surface adsorption of QA on scheelite in Fig. 12(a-II), in comparison with Fig. 12(b-II), the new separated peak of O1s which was C=O (-COOH) of QA was observed at ~533.40 eV on surface of calcite (Gao et al., 2018). These results showed that QA was liable to chemisorbed on the calcite surface and its functional group was mainly carboxyl. Fig. 13 given the situations about the high-resolution of XPS spectra of Ca2p on scheelite and calcite under the condition with QA and that without QA. The one double-peaks corresponding to Ca2p3/2 and Ca2p1/2 of $CaWO_4$ which was given by the fitted Ca2p peaks of scheelite was at ~346.93eV and ~350.49 eV in Fig. 13(a-I) (Luo et al., 2020). The one double-peaks corresponding to Ca2p3/2 and Ca2p1/2 of $CaCO_3$ of untreated calcite were found in Ca2p spectra (Fig. 13(b-I)) at ~347.15 eV and ~350.70 eV (Zhang and Ren et al., 2019). In the presence of QA, The Ca2p spectra of scheelite (Fig. 13(a-II)) showed that the binding energies didn't have evident shift which still were at ~346.89 eV for Ca2p3/2 and ~350.44 eV for Ca2p1/2. So the QA could be thought that it only played a slight role on the chemical environment on the scheelite surface because of the mild shifts of above energies. The new peaks for Ca2p3/2 and Ca2p1/2 on surface of calcite (Fig. 13(b-II)) were fitted at ~347.27 eV and ~350.98 eV after QA treatment, respectively, which was in correspondence with the -COO-Ca which formed with the calcium ions combining with -COOH in QA (Janusz and Skwarek, 2020; Ventruti et al., 2015). Therefore, QA could

have the selectivity to be restrain the calcite for its surface chemisorption on the calcite through the combination of oxygen atoms in carboxyl and Ca^{2+}.
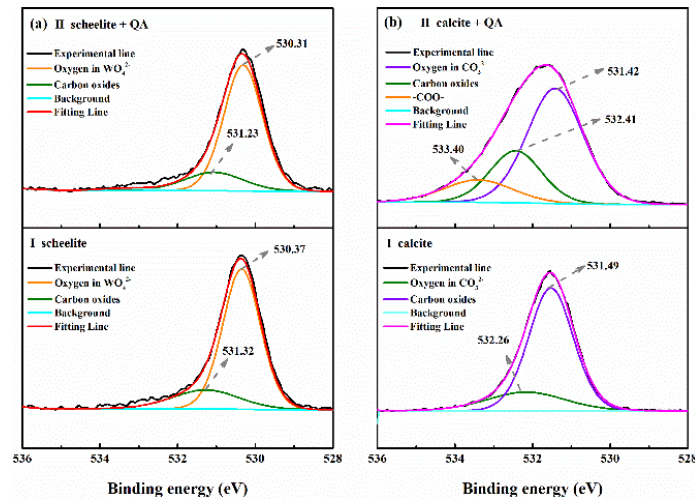
Fig. 10. XPS survey spectrum of scheelite(a) and calcite(b) before and after reaction with QA
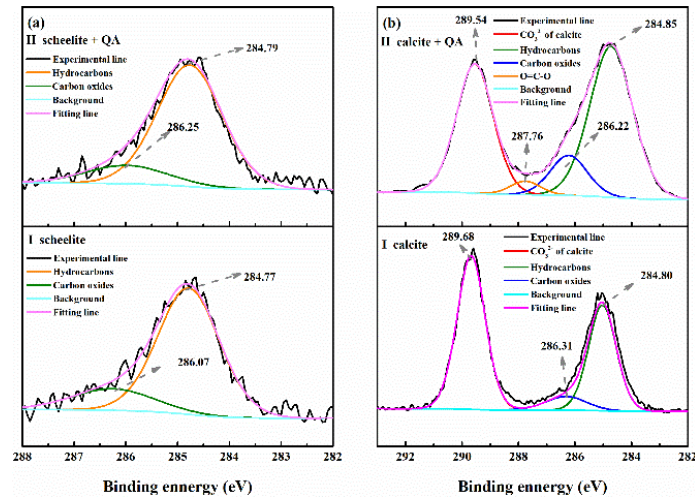
Fig. 11. High resolution spectra of C1s on the surface of scheelite (a) and calcite (b) before and after the reaction with QA
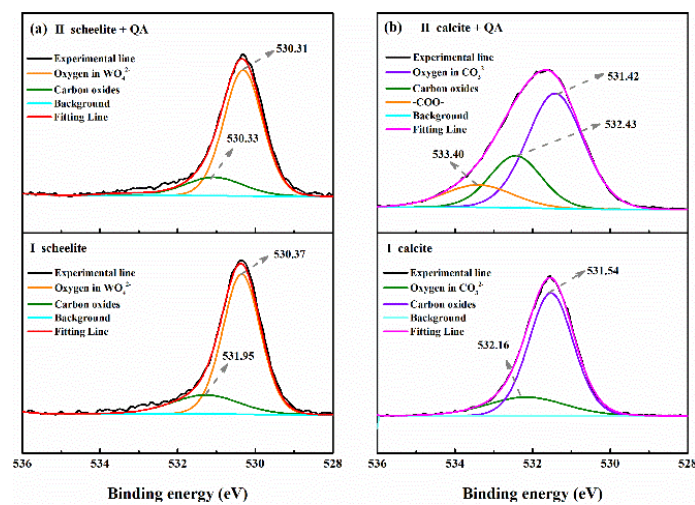
Fig. 12. High resolution spectra of O1s on the surface of scheelite (a) and calcite (b) before and after the reaction with QA
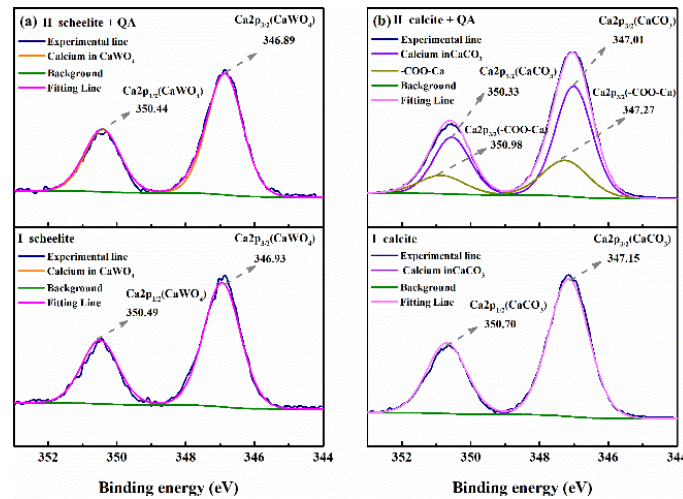
Fig. 13. High resolution spectra of Ca2p on the surface of scheelite (a) and calcite (b) before and after the reaction with QA

3.2.6. Crystal chemistry analysis

The cleavage surface is the crystal surface produced in the grinding process of minerals. The surface structure and atomic activity of the cleavage surface determine the reactivity of surface electricity, wettability and reagent adsorption, which affects the flotation behavior of minerals. Scheelite belongs to tetragonal system, and its main cleavage planes are (112), (001), (101) 103). Calcite belongs to the trigonal system, and the main cleavage plane are (104), (110), (001) (018) (Gao et al., 2017; Kuang et al., 2022). According to the active sites of calcium and the number of broken bonds in the unit cell of each crystal face of scheelite and calcite. The (112) surface was a common cleavage and exposed planes of scheelite. The calcium site of a unit cell of this crystal surface was 2 and the number of calcium points in the area of 1 nm² was 3.9738. The main cleavage and exposed surface of calcite was (104), which was 4.9505 of the number of calcium points within 1 nm² area. It could be seen that the number of calcium sites in the unit area of the main exposed surface (112) of scheelite was obviously smaller than that of the main exposed surface (104) of calcite. In addition, the number of calcium sites in the 1 nm² area of (101) and (103) planes of scheelite were also smaller than that of calcite (110) and (001) planes. Only the number of calcium sites in the 1nm² area of scheelite (001) plane was slightly higher than that of calcite (018), but the bonding force in the crystal structure of scheelite (001) plane was stronger, and it was less exposed in minerals. Therefore, the number of calcium sites in the unit area of calcite was generally higher than that of scheelite surface, indicating that the activity of calcite surface was higher than that of the surface. The number of calcium broken bonds in the 1 nm² area of (112) surface of scheelite is greater than that of (104) surface of calcite. However, according to the crystal structure of scheelite and calcite in Fig. 14, the number of calcium coordination in scheelite was 8, while that of calcite was 6. It was reported in the literature that QA and divalent metal ions generally have four or six coordination structures, and it was difficult to form an eight coordination structure (Inomata et al., 1999). Therefore, QA was difficult to react with the eight coordinated calcium site on the surface of scheelite, but easier to react with the six coordinated calcium site on the surface of calcite.

3.2. Adsorption model of quinic acid in flotation separation of scheelite from calcite

The selective adsorption model of QA on the scheelite and calcite surfaces was shown in Fig. 15. The negative charged tungstate ions (WO_4^{2-}) of scheelite surface were the primary component because the Ca^{2+} was preferentially dissolved in alkaline solution. By contrast, on the surface of calcite, CO_3^{2-} with negative points was preferentially dissolved, indicating its major components were chiefly positively charged calcium (Wang et al., 2021; Wei et al., 2019). The QA with negative charge which was electrostatically attracted to the mineral surface couldn't be adsorbed on scheelite surface with negative charge but could had adsorption on calcite surface with positive charge. According to the crystal

12

Physicochem. Probl. Miner. Process., 59(2), 2023, 166008

chemistry analysis, the number of calcium sites in the unit area of calcite was generally higher than that of scheelite surface, indicating that the activity of calcite surface was higher than that of the

Table 3. Calculation of surface broken bonds of scheelite and calcite

Minerals	Surface	Unit cell area (nm²)	Number of Ca in unit cell	Number of Ca per unit area (nm⁻²)	Number of Ca broken bond in unit cell	Number of Ca broken bond per unit area (nm⁻²)
scheelite	112	0.5033	2	3.9738	4	7.9475
	001	0.2749	1	3.6377	2	7.2754
	101	0.3559	1	2.8097	3	8.4293
	103	0.5271	2	3.7943	7	13.2802
calcite	104	0.4040	2	4.9505	2	4.9504
	110	0.5161	2	3.8752	4	7.7504
	001	0.2490	1	4. 0161	3	12.0483
	018	0.6412	2	3.1192	4	6.2384
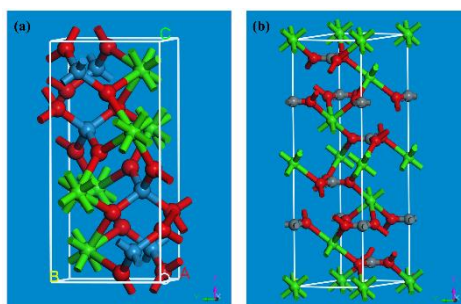
Fig. 14. The unit cell structure of scheelite (a) and calcite (b)

surface. QA was difficult to react with the eight coordinated calcium site on the surface of scheelite, but easier to react with the six coordinated calcium site on the surface of calcite. For the sake of the differences of localized ions types and the distance matched-degree of functional groups in QA and adjacent Ca^{2+} on the mineral surface, QA could have more chemisorption on the calcite than scheelite surface. Subsequently, the carboxyl group in QA further chelates with Ca^{2+} to take shape chemical layer adsorbents results in rendering the strong hydrophilic on calcite surface.

Because of its positive charge, the Pb-BHA which was added into the slurry of QA for pre-adsorption as the collector, would be prioritized to adsorb on the scheelite surface which had negative charge, whose lead group would appear chemisorption via acting with the oxygen atoms, resulting in enhanced surface hydrophobicity of scheelite. The Pb-BHA complex would form interfaced co-adsorption with foaming agent assembly which is beneficial to greatly reduce surface tension of the solution and come into being a stabilized foam layer. It's wroth noting that the Pb-BHA complex hardly had adsorption on the calcite surface because the surface active site was occupied by QA which hindered the adsorption of Pb-BHA, so that the calcite wasn't able to form adhesion on the bubble and still kept its hydrophilic and gone down to the bottom of the slurry, conversely, the scheelite could have the adhesion with the air bubbles to form a steady froth layer and floatation.

4. Conclusions

Quinic acid was a non-toxic, environmentally friendly, efficient depressant which could make the scheelite flotation separate from calcite. As the concentration of QA was 1.5×10^{-4} mol·L-1at pH=9.0, the
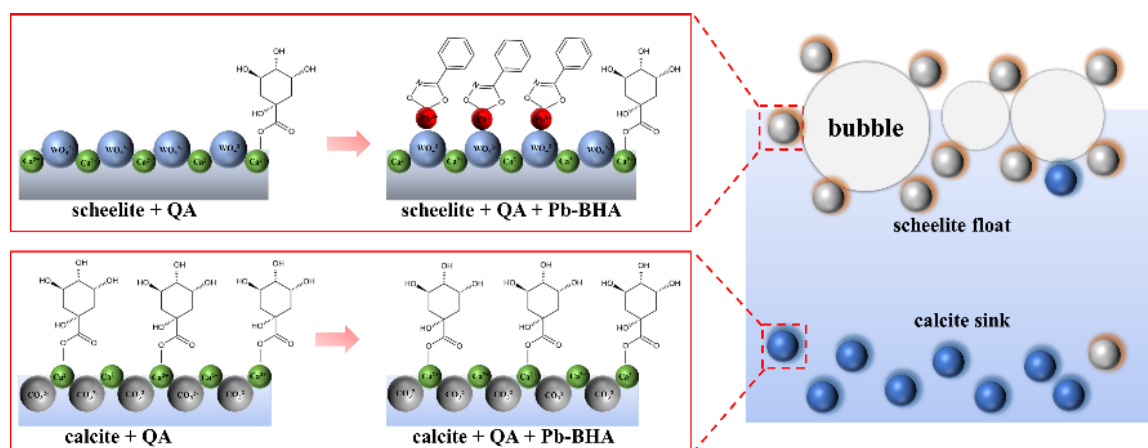
Fig. 15. Selective adsorption model of QA in scheelite and calcite flotation

recovery rate of scheelite was higher than 95% but that of calcite was only 18.02%. Artificial mixed mineral experiment could obtain tungsten concentrate with high grade and high recovery, the best separating results were obtained with 1.5×10^{-4} mol·L^{-1} QA at pH=9, with 66.24% WO$_3$ grade and 89.46%WO$_3$ recovery of the tungsten concentrate.

The number of calcium sites in the unit area of calcite was generally greater than that of scheelite surface, and QA was more effortless to react with the six coordinated calcium site on the surface of calcite than that with the eight on scheelite. Moreover, the Ca^{2+} of the calcite and WO$_4^{2-}$ of scheelite were respectively the major component on their surface. QA with negative charge preferred to have surface adsorption on the calcite with positive charge through electrostatic attraction rather than scheelite with the negative charge. Subsequently, the carboxyl group of depressant QA farther chelated with Ca^{2+}, so that a good deal of QA was took place chemical adsorption on the surface of calcite to enhance its hydrophilicity, while there was hardly adsorption of QA, which had less affected on the wettability of scheelite surface. After treating continuously by Pb-BHA, QA was largely adsorbed on the calcite surface and occupied most of the calcium ion species, which prevented the adsorption of Pb-BHA on that.

Acknowledgments

References

ABDALLA, M. A. M., PENG, H., YOUNUS, H. A., ET AL., 2018. *Effect of synthesized mustard soap on the scheelite surface during flotation.* Colloids Surf. A, 548, 108-116.

ALLEGRETTI, Y., FERRER, E. G., BARO´, A. C. G., ET AL., 2000. *Oxovanadium (IV) complexes of quinic acid. Synthesis, characterization and potentiometric study*, Polyhedron. 19, 2613-2619.

CHEN, P., ZHAI, J., SUN, W., ET AL., 2017. *The activation mechanism of lead ions in the flotation of ilmenite using sodium oleate as a collector.* Miner. Eng. 111, 100-107.

CHEN, W., FENG, Q., ZHANG, G., ET AL., 2018. *Investigations on flotation separation of scheelite from calcite by using a novel depressant: Sodium phytate.* Miner. Eng. 126, 116-122.

CLIFFORD, M. N., JAGANATH, I. B., LUDWIG, I. A., ET AL., 2017. *Chlorogenic acids and the acyl-quinic acids: discovery, biosynthesis, bioavailability and bioactivity.* Nat. Prod. Rep. 34, 1391-1421.

DENG, R., YANG, X., HU, Y., ET AL., 2018. *Effect of Fe(II) as assistant depressant on flotation separation of scheelite from calcite.* Miner. Eng. 118, 133-140.

DONG, L., JIAO, F., QIN, W., ET AL., 2019a. *Activation effect of lead ions on scheelite flotation: Adsorption mechanism, AFM imaging and adsorption model*. Sep. Purif. Technol. 209, 955-963.

DONG, L., JIAO, F., QIN, W., ET AL., 2018. *New insights into the carboxymethyl cellulose adsorption on scheelite and calcite: adsorption mechanism, AFM imaging and adsorption model*. Appl. Surf. Sci. 463, 105-114.

DONG, L., JIAO, F., QIN, W., ET AL., 2019b. *Selective depressive effect of sodium fluorosilicate on calcite during scheelite flotation.* Miner. Eng. 131, 262-271.

DONG, L., JIAO, F., QIN, W., ET AL., 2019c. *Selective flotation of scheelite from calcite using xanthan gum as depressant.* Miner. Eng. 138, 14-23.

DONG, L., JIAO, F., QIN, W., ET AL., 2021a. *New insights into the depressive mechanism of citric acid in the selective flotation of scheelite from fluorite*. Miner. Eng. 171, 107-117.

DONG, L., JIAO, F., QIN, W., ET AL., 2021b. *Utilization of iron ions to improve the depressive efficiency of tartaric acid on the flotation separation of scheelite from calcite*. Miner. Eng. 168, 106925.

ESPIRITU, E. R. L., NASERI, S., WATERS, K. E., .2018. *Surface chemistry and flotation behavior of dolomite, monazite and bastnasite in the presence of benzohydroxamate, sodium oleate and phosphoric acid ester collectors.* Colloids Surf. A, 546, 254-265.

FENG, B., PENG, J., ZHANG, W., ET AL., 2018. *Use of locust bean gum in flotation separation of chalcopyrite and talc.* Miner. Eng. 122, 79-83.

FOUCAUD, Y., FILIPPOVA, I. V., FILIPPOV, L. O., 2019. *Investigation of the depressants involved in the selective flotation of scheelite from apatite, fluorite, and calcium silicates: Focus on the sodium silicate/sodium carbonate system.* Powder Technol. 352, 501-512.

FU, J., HAN, H., WEI, Z., ET AL., 2021. *Selective separation of scheelite from calcite using tartaric acid and Pb-BHA complexes*. Colloids Surf. A, 622, 126657.

GABRIEL, C., MENELAOU, M., DASKALAKIS, M., ET AL., 2008. *Synthetic, structural, spectroscopic and solution speciation studies of the binary Al(III)-quinic acid system. Relevance of soluble Al(III)-hydroxycarboxylate species to molecular toxicity.* Polyhedron, 27, 2911-2920.

GAO, Y., GAO, Z., SUN, W., ET AL., 2016. *Selective flotation of scheelite from calcite: a novel reagent scheme*. Int. J. Miner. Process. 154, 10-15.

GAO, Z., LI, C., SUN, W., ET AL., 2017. *Anisotropic surface properties of calcite: A consideration of surface broken bonds.* Colloids Surf. A, 520, 53-61.

GAO, Z., WANG, Z., CHANG, J., ET AL., 2019. *Micelles directed preparation of ternary cobalt hydroxide carbonate-nickel hydroxide-reduced graphene oxide composite porous nanowire arrays with superior faradic capacitance performance.* J. Colloid Interf. Sci. 534, 563-573.

GONG, D., ZHANG, Y., WAN, L., ET AL., 2022. *Efficient extraction of tungsten from scheelite with phosphate and fluoride.* Process. Saf. Environ. 159, 708-715.

HAN, G., WEN, S., WANG, H., ET AL., 2020. *Selective adsorption mechanism of salicylic acid on pyrite surfaces and its application in flotation separation of chalcopyrite from pyrit*e. Sep. Purif. Technol. 240, 116650.

HAN, H. HU, Y., SUN, W., ET AL., 2018, *Novel catalysis mechanisms of benzohydroxamic acid adsorption by lead ions and changes in the surface of scheelite particles*. Miner. Eng. 119, 11-22.

HAN, H., XIAO, Y., HU, Y., ET AL., 2020. *Replacing Petrov's process with atmospheric flotation using Pb-BHA complexes for separating scheelite from fluorite*. Miner. Eng. 145, 106053.

HOLMSTEDT, S., EFIMOV, A., CANDEIAS, N. R., 2021. O, *O-silyl group migrations in quinic acid derivatives: an opportunity for divergent synthesis*. Org. Lett. 23, 3083-3087.

INOMATA, Y., HANEDA, T., HOWELL, F.S., 1999. *Characterization and crystal structures of zinc(II) and cadmium(II) complexes with D-()-quinic acid.* J. Inorg. Biochem. 76, 13-17.

JANUSZ, W., SKWAREK, E., 2020. *Comparison of oxalate, citrate and tartrate ions adsorption in the hydroxyapatite/aqueous electrolyte solution system*. Colloids Interface. 4.

JIAO, F., DONG, L., QIN, W., ET AL., 2019. *Flotation separation of scheelite from calcite using pectin as depressant*. Miner. Eng. 136, 120-128.

JIN, E. S., YANG, F., ZHU, Y. Y., ET AL., 2016. *Surface characterizations of mercerized cellulose nanocrystals by XRD, FT-IR and XPS*. J. Cellulose Sci. Technol. (Chinese)

KALPAKLI, A. O., ILHAN, S., KAHRUMAN, C., ET AL., 2012. *Dissolution behavior of calcium tungstate in oxalic acid solutions.* Hydrometallurgy. 121-124, 7-15.

KANG, J., HU, Y., SUN, W., ET AL., 2019. Utilization of sodium hexametaphosphate for separating scheelite from calcite and fluorite using an anionic-nonionic collector. Minerals. 9, 705-721.

KANG, J., KHOSO, S. A., HU, Y., ET AL., *Utilisation of 1-Hydroxyethylidene-1, 1-diphosphonicacid as a selective depressant for the separation of scheelite from calcite and fluorite.* Colloids Surf. A 582 (2019), 123888.

KATELNIKOVAS, A., GRIGORJEVA, L., MILLERS, D., ET AL., 2017. *Sol-gel preparation of nanocrystalline CaWO4.* Lith. J. Phys. 47, 63-68.

KUANG, J., WANG, X., YU, M., ET AL., 2022. *Flotation behavior and mechanism of calcium carbonate polymorphs with sodium oleate as collector.* Powder Technol. 398, 117040.

KUPKA, N., RUDOLPH, M., 2018, *Froth flotation of scheelite - A review.* Int. J. Min. Sci. Techno. 28, 373-384.

LI, H., ZHANG, S., JIANG, H., ET AL., 2011. *Effect of degree of substitution of carboxymethyl starch on diaspore depression in reverse flotation.* T. Nonferr. Metal. Soc. 8, 1868-1873.

Liu, C., Ni, C., Yao, Chang, J. Z., ET AL., 2021. *Hydroxypropyl amine surfactant: A novel flotation collector for efficient separation of scheelite from calcite.* Miner. Eng. 167, 106898.

LIU, J., WANG, X., ZHU, Y., ET AL., 2022. *Flotation separation of scheelite from fluorite by using DTPA as a depressant.* Miner. Eng. 175 107311.

LIU, X., HUANG, G., LI, C., ET AL., 2015. *Depressive effect of oxalic acid on titanaugite during ilmenite flotation.* Miner. Eng. 79, 62-67.

LU, Y. L., LIU, D. W., JIA, X. D., ET AL., 2014. *A review on flotation process of scheelite.* Adv. Mater. Research. 962-965, 388-392.

LUO, Y., ZHANG, G., MAI, Q., ET AL., 2019. *Flotation separation of smithsonite from calcite using depressant sodium alginate and mixed cationic/anionic collectors.* Colloids Surf. A. 586, 124227.

MARTINS, J. G., CAMARGO, S. E. A., BISHOP, T. T., A. F. MARTINS, ET AL., 2018., *Pectin-chitosan membrane scaffold imparts controlled stem cell adhesion and proliferation.* Carbohyd. Polym. 197, 47-56.

NURI, O. S., IRANNAJAD, M., MEHDILO, A., 2019. *Effect of surface dissolution by oxalic acid on flotation behavior of minerals.* J. Mater. Res. Technol. 8, 2336-2349.

SALDYKA, M., COUSSAN, S., 2020. *Infrared spectra and photodecomposition of benzohydroxamic acid isolated in argon matrices.* J. Mol. Struct. 1219, 128506.

SAMIMI, S., ARDESTANI, M. S., DORKOOSH, F. A., 2021. *Preparation of carbon quantum dots - quinic acid for drug delivery of gemcitabine to breast cancer cells.* J. Drug. Deliv. Sci. Tec. 61, 102287

SARQUÍS, P. E., MENENDEZ-AGUADO, J. M., MAHAMUD, M. M., ET AL., 2014. *Tannins: the organic depressants alternative in selective flotation of sulfides.* J. Clean. Prod. 84, 723-726.

SHEPETA, E. D., SAMATOVA, L. A., KONDRAT'EV, S. A., 2012. *Kinetics of calcium minerals flotation from scheelite-carbonate ore*s. J. Min. Sci. 48, 746-753.

VENTRUTI, G., SCORDARI, F., BELLATRECCIA, F., ET AL., 2015. *Calcium tartrate esahydrate, CaC4H4O6·6H2O: a structural and spectroscopic study.* Acta Crystallogr. Sect. B. 71, 68-73.

WANG, C., REN, S., SUN, W., ET AL., 2021. *Selective flotation of scheelite from calcite using a novel self-assembled collector.* Miner. Eng. 171, 107120.

WANG, J., BAI, J., YIN, W., ET AL., 2018. *Flotation separation of scheelite from calcite using carboxyl methyl cellulose as depressant.* Miner. Eng. 127, 329-333.

WANG, X., JIA, W., YANG, C., ET AL., 2021. *Innovative application of sodium tripolyphosphate for the flotation separation of scheelite from calcite.* Miner. Eng. 170, 106981.

WEI, Z. FU, J., HAN, H., ET AL., 2020. *A highly selective reagent scheme for scheelite flotation: polyaspartic acid and Pb-BHA complexes.* Minerals, 10, 561.

WEI, Z. HU, Y., HAN, H., ET AL., 2019. *Selective separation of scheelite from calcite by self-assembly of H2SiO3 polymer using Al3+ in Pb-BHA flotation.* Minerals, 9(1).

WEI, Z. SUN, W. WANG, P. ET AL., 2021. *A novel metal-organic complex surfactant for high-efficiency mineral flotation.* Chem. Eng. J. 426, 130853.

WEI, Z., HU, Y., HAN, H., ET AL., 2018. *Selective flotation of scheelite from calcite using Al-Na2SiO3 polymer as depressant and Pb-BHA complexes as collector.* Miner. Eng. 120, 29-34.

YANG, X., 2018. *Beneficiation studies of tungsten ores - A review.* Miner. Eng. 125, 111-119.

YAO, W., LI, M., ZHANG, M., ET AL., 2022. *Effects of Pb2+ ions on the flotation behavior of scheelite, calcite, and fluorite in the presence of water glass.* Colloids and Surfaces A: Physicochemical and Engineering Aspects 632.

ZHANG, C., HU, Y., W. SUN, ET AL., 2019, *Effect of phytic acid on the surface properties of scheelite and fluorite for their selective flotation.* Colloids Surf. A. 573, 80-87.

ZHANG, C., SUN, W., HU, Y., ET AL., 2018. *Selective adsorption of tannic acid on calcite and implications for separation of fluorite minerals*. J. Colloid. Interf. Sci. 512, 55-63.

ZHANG, W., HONAKER, R. Q., 2018. *Flotation of monazite in the presence of calcite part II: Enhanced separation performance using sodium silicate and EDTA*. Miner. Eng. 127, 318-328.